

UDC 539.3

INFLUENCE OF MASS ON THE EFFICIENCY AND DYNAMICS OF SINGLE-SIDED AND DOUBLE-SIDED VIBRO-IMPACT NONLINEAR ENERGY SINKS

P.P. Lizunov

O.S. Pogorelova

T.G. Postnikova

O.V. Gerashchenko

*Kyiv National University of Construction and Architecture
31, Povitryanykh Syl ave., Kyiv, Ukraine, 03680*

DOI: 10.32347/2410-2547.2024.113.3-17

The efficiency of the asymmetric single-sided and symmetric double-sided vibro-impact nonlinear energy sinks, that is, vibro-impact dampers, for mitigating unwanted vibrations of the main structure are quite high and similar for dampers with different masses and designs. However, its dynamic behavior is different. The optimal design of the dampers with lower mass has unusual, “strange” parameter set. The regions of bilateral damper impacts on the both barriers are narrow and located near the resonant frequency of the exciting force.

Keywords: nonlinear energy sink, damper, vibro-impact, single-sided, double-sided, optimization, bilateral impacts.

1. Introduction

This paper discusses the problem of mitigating undesirable vibrations of a heavy main structure. One of the ways to solve it is the use of active, hybrid and passive vibration control devices. Passive control devices have the advantage of having no additional power source. Due to the development of nonlinear methods and related software, nonlinear passive vibration control devices have been proposed after extensive discussion and application of linear devices such as Tuned Mass Dampers (TMD) [1, 2]. The devices attached to the main structure using nonlinear coupling have been widely discussed during the last two decades. They have been called Nonlinear Energy Sinks because their discussion began within the framework of the idea of Targeted Energy Transfer (TET) [3]. This idea states that such dampers, due to their nonlinearity, take away the part of the main structure energy and thus reduce its energy [4, 5].

The world scientific literature proposes many different types of NESs. The vibro-impact nonlinear energy sink (VI NES), that is, the vibro-impact damper, is one of them [6, 7, 8]. The VI NESs are considered to be a fairly effective type [9, 10, 11]. When considering the VI NES problem, finding its optimal design is of paramount importance. The optimal damper design, that is, a set of its parameters, should provide the best mitigation of the main structure vibrations. However, this task is complex and ambiguous. Optimization procedures do not and cannot give an unambiguous result, since there are many damper parameter sets that provide the similar mitigation of the main structure vibrations [12]. This article shows this phenomenon very clearly. We perform optimization procedures using standard software, namely MATLAB platform tools. It is worth noting that the optimization procedure itself allows for the great arbitrariness [13]. Its execution requires a great experience and skill from the performer.

The problem of impact modeling is an important one in studying the vibro-impact system dynamics. After detailed examining this problem [14, 15], we simulate an impact using the interactive contact force according to the quasi-static Hertz's contact theory [16, 17].

In this paper, we consider two classical types of VI NESs, namely asymmetric single-sided and symmetric double-sided (SSVI NES and DSVI NES). They differ only in geometry, more precisely the layout of the obstacles, and have the same mechanics. The system strong nonlinearity and discontinuity are due to the repeated damper impacts on the obstacles. In SSVI NES model, it hits directly the PS, which is the left barrier in its oscillatory motion, and the right obstacle. In DSVI NES model the damper hits the left and right obstacles. In the search for an optimal damper design, we do not include

its mass in the list of optimized parameters and search for an optimal set of damper parameters separately for each predetermined mass. The paper analyzes the influence of damper mass on its efficiency in mitigating the main structure vibrations and on the system dynamic behavior.

Our previous work [18] studied in detail the system dynamic behavior and the efficiency of the damper with mass 40 kg. This paper has an extensive bibliography.

So, the goals of this article are as follows:

- find the sets of optimal damper parameters for both models and for each chosen damper mass;
- compare the efficiency of both damper models in mitigating vibrations of the main structure for each chosen damper mass;
- show and compare the dynamic behavior of both damper models for each chosen mass when the exciting force frequency is changed;
- show the effect of changing the damper mass on its efficiency and system dynamic behavior.

2. Model description and governing equations

In this paper, we study the dynamic behavior of a two-mass vibro-impact system with two-degrees-of-freedom consisting of a main body (primary structure - PS) and a vibro-impact damper attached to it. We study the efficiency of the damper in mitigating the PS vibrations. The dependence of damper efficiency and system dynamic behavior on the mass of the damper with other optimized parameters is also studied. A vibro-impact damper is a nonlinear energy sink (NES). Two damper types are considered in this paper, namely asymmetric single-sided and symmetric double-sided vibro-impact NESs – SSVI NES and DSVI NES. Their conceptual schemes are presented in Fig.1. They differ only in geometry, namely in obstacle layout; the mechanical connections are the same. The symmetry of the double-sided VI NES is also only geometrical. Dampers of greater mass make symmetrical impacts on the both obstacles, but the symmetry of the impacts is broken for dampers with lower mass.

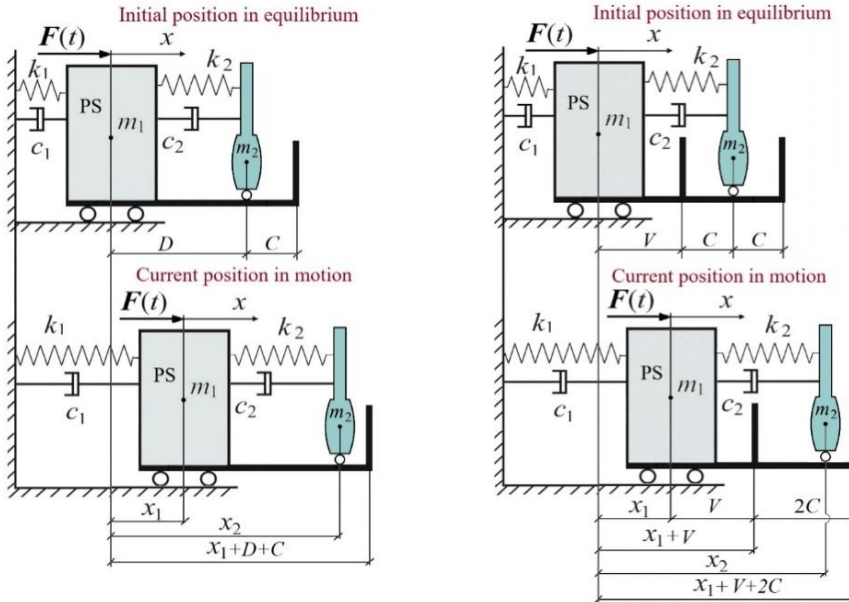


Fig. 1. Conceptual schemes of asymmetric single-sided VI NES; symmetric double-sided VI NES

The designations of mechanical connections, masses of both bodies, and distances are shown in Fig. 1. The damper mass is much less than the PS mass $m_2 \ll m_1$. The PS is under the action of an external load $F(t)$, which is a harmonic force in this paper

$$F(t) = P \cos(\omega t + \varphi_0), P = 800 \text{ N. Its period is } T = 2\pi/\omega. \quad (1)$$

The parameters of the primary structure are set in advance and are not subject to optimization in this paper. We set them up as follows: $m_1 = 1000 \text{ kg}$, $k_1 = 3.95 \cdot 10^4 \text{ N/m}$, $c_1 = 452 \text{ N}\cdot\text{s/m}$.

The problem of impact modeling is very important in the study of vibro-impact system movement. After examining this problem, we in all our works simulate an impact using interactive nonlinear contact force according to quasi-static Hertz contact theory

$$F_{con}(z) = K[z(t)]^{3/2}. \quad (2)$$

The impact is not instantaneous; it has some duration. Hertz's theory allows for local deformations in the contact zone. In formula (2), z is the colliding bodies' rapprochement in the contact zone due to local deformation. This rapprochement caused by an impact may be written through distance specifications. Naturally, the rapprochements for left and right impacts are different. The left impact is a damper impact on the PS directly for SSVI NES and on the left obstacle for DSVI NES. The right impact is a damper impact on the right obstacle for both damper types.

The left impacts occur when

$$x_1 \geq x_2, \\ \text{i.e. } (x_1 - x_2) \geq 0$$

then the rapprochements are

$$z_1 = x_1 - x_2$$

for SSVI NES

$$x_2 \leq (x_1 + V), \\ \text{i.e. } (x_1 - x_2 + V) \geq 0$$

then the rapprochements are

$$z_1 = x_1 - x_2 + V.$$

The right impacts occur when

$$x_2 \geq (x_1 + D + C), \\ \text{i.e. } (x_2 - x_1 - D - C) \geq 0$$

$$z_2 = x_2 - x_1 - D - C$$

for DSVI NES

$$x_2 \geq (x_1 + V + 2C), \\ \text{i.e. } [x_2 - x_1 - (V + 2C)] \geq 0$$

$$z_2 = x_2 - x_1 - (V + 2C).$$

The coefficient K in formula (2) characterizes the mechanical and geometric properties of colliding surfaces. Therefore, it also differs for damper impacts on the left obstacle (or PS directly) and on the right obstacle:

When impacting the left obstacle (or PS directly)

$$K_1 = \frac{4}{3} \frac{q_1}{(\delta_1 + \delta_2) \sqrt{A_1 + B_1}}, \\ \delta_1 = \frac{1 - \nu_1^2}{E_1 \pi}, \quad \delta_2 = \frac{1 - \nu_2^2}{E_2 \pi}.$$

When impacting the right obstacle

$$K_2 = \frac{4}{3} \frac{q_2}{(\delta_3 + \delta_4) \sqrt{A_2 + B_2}}, \\ \delta_3 = \frac{1 - \nu_3^2}{E_3 \pi}, \quad \delta_4 = \frac{1 - \nu_4^2}{E_4 \pi}. \quad (3)$$

Here the Young's moduli of elasticity for all surfaces E_1, E_2, E_3, E_4 and Poisson's ratios $\nu_1, \nu_2, \nu_3, \nu_4$ are included into the characteristics of colliding surfaces. The values E_1 and ν_1 characterize the contact surface of the left barrier, i.e. the PS or the left obstacle; the values E_3 and ν_3 – the contact surface of the right obstacle; the values E_2, E_4 and ν_2, ν_4 – the left and right contact surfaces of the vibro-impact damper. We considered the values E_1, E_3 and ν_1, ν_3 as predetermined and did not optimize them:

$$E_1 = E_3 = 2.1 \cdot 10^{11} \text{ N/m}^2, \quad \nu_1 = \nu_3 = 0.3.$$

The values E_2, E_4 and ν_2, ν_4 were included in the list of optimized parameters. There were obtained the system responses to their changes. This made it possible to analyze the effect of changing the mechanical characteristics of colliding surfaces in more detail than the more prevalent consideration of the experimental restitution coefficient [19]. The results of their optimization will be shown in next Sec. 3.

Then the motion equations for this system are as follows:

$$m_1 \ddot{x}_1 + c_1 \dot{x}_1 + k_1 x_1 - c_2 (\dot{x}_2 - \dot{x}_1) - k_2 (x_2 - x_1 - D) = F(t) - H(z_1) F_{con}(z_1) + H(z_2) F_{con}(z_2), \\ m_2 \ddot{x}_2 + c_2 (\dot{x}_2 - \dot{x}_1) + k_2 (x_2 - x_1 - D) = H(z_1) F_{con}(z_1) - H(z_2) F_{con}(z_2). \quad (4)$$

The initial conditions are

for SSVI NES

at $t = 0$, we have

$$\begin{aligned}x_1(0) &= 0, \quad x_2(0) = D, \\ \dot{x}_1(0) &= \dot{x}_2(0) = 0, \quad \varphi_0 = 0.\end{aligned}$$

for DSVI NES

at $t = 0$, we have

$$\begin{aligned}x_1(0) &= 0, \quad x_2(0) = V + C, \\ \dot{x}_1(0) &= \dot{x}_2(0) = 0, \quad \varphi_0 = 0.\end{aligned}$$

The presence of the discontinuous Heaviside step function $H(z)$ in the motion equations (4) makes the set of the Ordinary Differential Equations (ODE) stiff one. The integration step of a stiff system should not only be variable, but also extremely small at the impact points. For integrating this system, we use MATLAB stiff ODE solver *ode23s*. This variable-step solver allows us to determine with sufficient accuracy the instant when the Heaviside function $H(z)$ becomes equal to unity, that is, in our problem the collision of the bodies begins.

Integration of the motion equations (4) determines the displacements and the velocities of both bodies, which allow us to calculate the total mechanical energy of the primary structure using the well-known formula:

$$E_{total}(t) = E_{kinetic}(t) + E_{poten}(t) = \frac{m_1 \dot{x}_1(t)^2 + k_1 x_1(t)^2}{2}. \quad (5)$$

Its maximum value is chosen as the objective function for the optimization procedures.

3. Optimization of damper parameters

The world scientific literature as well as our studies and calculations insist that optimizing the damper parameters to maximize its effectiveness for mitigating the PS vibrations is a necessary and important procedure. Mitigating the PS vibrations means reducing its maximum displacements and velocities. Therefore, it is reasonable to evaluate the reduction of the maximum total mechanical energy of the PS, which is calculated by the formula (5). This evaluation is in line with the idea of Targeted Energy Transfer (TET), under which the NESs are studied. According to this idea, the NES, due to its nonlinearity, takes away some of the PS energy and consequently reduces its energy. So, it is reasonable to choose the maximum total energy of the PS E_{1max} as the objective function and search for such values of damper parameters that ensure its minimal value. In our previous work [20], we showed that the choice of parameters for its calculation is also important. It was shown that the exciting force frequency, at which the objective function is calculated, should be close to the resonant one. We calculate it at $\omega = 6.3$ rad/s.

We use standard software for minimizing the objective function, namely the *surface* and *fminsearch* programs from the MATLAB platform. Program *surface* allows us to get an initial assessment for various parameters. Program *fminsearch* searches for local minima of the objective function and allows simultaneous optimization of several parameters. Our methodology for performing optimization procedures has been described in detail in our previous papers [18, 21]. In these works, it has been shown that a softer impact provides a better reduction of E_{1max} . There were found the optimal values of the Young's moduli $E_2 = 2.21 \cdot 10^7$ N/m², $E_4 = 2.05 \cdot 10^7$ N/m², which is consistent with suggestions to use a smaller value of Newtonian restitution coefficient when recording the velocity jump using this coefficient in impact modeling [22-24].

The scientific literature often recommends including the damper mass m_2 into the list of optimized parameters. However, the optimization programs show that a larger damper mass provides a smaller objective function value for the similar values of other parameters. Table 1 summarizes these values for DSVI NES.

Table 1

The results of simultaneous optimization of five parameters for DSVI NES

| V_{opt} , m | C_{opt} , m | c_{2opt} , N·s/m | k_{2opt} , N/m | m_{2opt} , kg | E_{1max} , J |
|---------------|---------------|--------------------|------------------|-----------------|----------------|
| 0.496 | 0.238 | 64.8 | 217 | 40.0 | 517 |
| 0.416 | 0.256 | 70.2 | 196 | 49.3 | 282 |
| 0.154 | 0.250 | 71.9 | 223 | 66.1 | 101 |

Therefore, we believe that the VI NES mass m_2 should not be optimized. The mass value must be selected in advance, and all other parameters must be optimized for this selected mass. For example, in [19], the authors construct the contour plots for each mass separately. In this paper, we analyze the efficiency and dynamic performance of the systems with attached SSVI NES and DSVINES of 4 different mass values: $m_2 = 60$ kg, 40 kg, 20 kg, and 10 kg, which are 6%, 4%, 2%, and 1% of the PS mass m_1 .

It is worth emphasizing that optimization procedures do not and cannot give the unambiguous result, since there are many sets of damper parameters that provide the similar minimal values of the objective function, that is, the similar mitigating the PS vibrations. This paper shows this very clearly. In the paper [12], the authors write: “*The nonlinear stiffness properties have significant influence on control effectiveness, and they can be implemented in numerous scenarios with plenty of configuration parameters.*” Besides, there is no rule or order for performing optimization procedures. In the article [13], the authors claim: “*There is no exact method to simplify the design of the multiparameter nonlinear energy sinks*”. The optimization of damper parameters requires a great experience and skill on the part of the researcher.

4. Dynamic behavior of the system with attached dampers of mass $m_2 = 60$ kg

This mass m_2 is 6% of the primary structure mass m_1 .

Optimization procedures allowed us to find five variants of the parameter sets for both SSVI NES and DSVI NES that provide good mitigation of the PS vibrations. Table 2 shows these parameters. The Table 2 also shows the values of the maximum total energy $E_{1\max}$ of the PS at the exciting force frequency $\omega = 6.3$ rad/s. This is the resonant frequency for the PS without any damper. In this case, the maximum total energy of the PS $E_{1\max} = 1557$ J. The rows with general title “Regimes” demonstrate the modes occurring in the system with different attached dampers. Hereinafter, the following notations are adopted. The designation nT, k, m indicates the nT -periodic mode (where T is the period of the harmonic exciting force) with k left impacts per cycle on the PS directly for the SSVI NES or on the left obstacle for the DSVI NES and m impacts on the right obstacle. For example, $2T, 1, 0$ is the regime of $2T$ periodicity with one impact per cycle on the left barrier and no impacts on the right obstacle. The AM designation indicates the amplitude-modulated mode, which will be discussed in detail below.

Table 2

Information about 5 variants of SSVI NES and DSVI NES of mass $m_2 = 60$ kg with optimized design

| Parameters | Variant | | | | | | | | | |
|---|--|--|--|--|--|------------------------|------------------------|------------------------|------------------------|------------------------|
| | SS-1(60) | SS-2(60) | SS-3(60) | SS-4(60) | SS-5(60) | DS-1(60) | DS-2(60) | DS-3(60) | DS-4(60) | DS-5(60) |
| k_2 , N/m | 215 | 215 | 227 | 203 | 215 | 218 | 236 | 260 | 237 | 561 |
| c_2 , N·s/m | 232 | 232 | 152 | 83.6 | 250 | 247 | 214 | 108 | 209 | 32.8 |
| $D(V)$, m | 0.0600 | 0.0600 | 0.0697 | 0.759 | 0.0600 | 0.0636 | 0.0608 | 0.0598 | 0.635 | 0.0505 |
| C , m | 0.300 | 0.360 | 0.349 | 0.435 | 0.300 | 0.149 | 0.182 | 0.222 | 0.189 | 0.268 |
| $E_{1\max}$, J at $\omega = 6.3$ rad/s | 321 | 570 | 241 | 145 | 335 | 379 | 303 | 206 | 761 | 135 |
| Regimes | $T, 0, 0$ $3T, 1, 0$ $2T, 1, 0$ $T, 1, 1$ AM | $T, 0, 0$ $3T, 1, 0$ $2T, 1, 0$ $T, 1, 1$ AM | $T, 0, 0$ $3T, 1, 0$ $2T, 1, 0$ $T, 1, 1$ AM | $T, 0, 0$ $3T, 1, 0$ $2T, 1, 0$ $T, 1, 1$ AM | $T, 0, 0$ $3T, 1, 0$ $2T, 1, 0$ $T, 1, 1$ AM | $T, 0, 0$ $T, 1, 1$ |

Fig. 2 presents the dependence of the maximum total energy $E_{1\max}$ of the PS on the exciting force frequency for these five variants. Fig. 2 clearly demonstrates the good mitigation of the PS vibrations similar for SSVI NES and for DSVI NES. Below we take a closer look at some of the features of these options. Table 2 shows the presence of $T, 0, 0$ regimes for all damper variants. This is a shockless regime without any impact. Fig. 3 and Fig. 4 give a clear indication of where the impacts are occurring. The pink zones bounded by the vertical dashed lines in both Figures are areas where the bilateral impacts occur. These are the direct impacts on the PS for the SSVI NES and the impacts on the left obstacle for the DSVI NES and impacts on the right obstacles for both damper types. Table 2 shows

that the regimes with bilateral impacts are $T,1,1$ for both damper types. However, amplitude-modulated (AM) regime with bilateral impacts also occur for SSVI NES. The light green areas in Fig. 3 correspond to the areas where the unilateral direct impacts on the PS occur. The white areas in both Figures indicate shockless movement $T,0,0$.

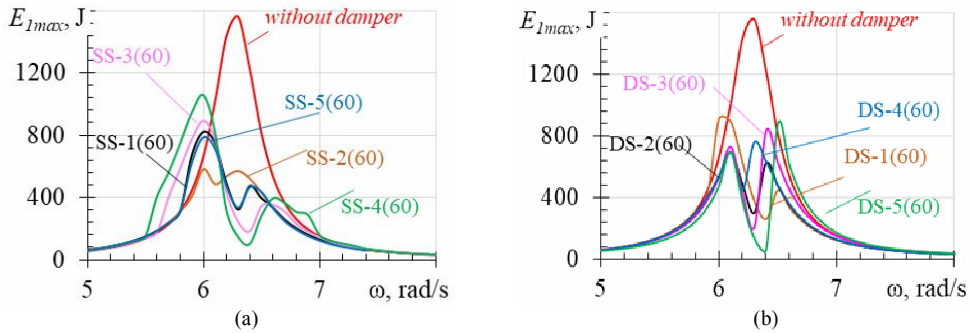


Fig. 2. The maximum total energy of the PS with different attached dampers of mass $m_2 = 60$ kg depending on the exciting force frequency: (a) for SSVI NES; (b) for DSVI NES

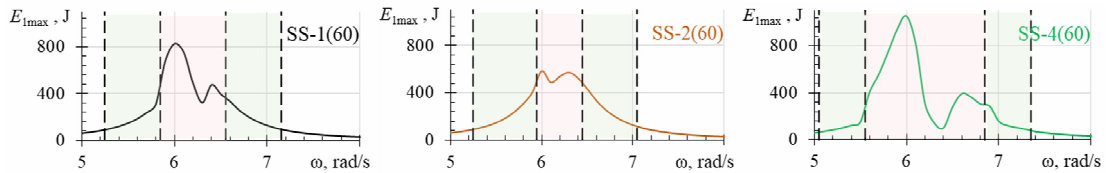


Fig. 3. The areas of bilateral and unilateral impacts for different single-sided vibro-impact nonlinear energy sinks with mass $m_2 = 60$ kg depending on the exciting force frequency

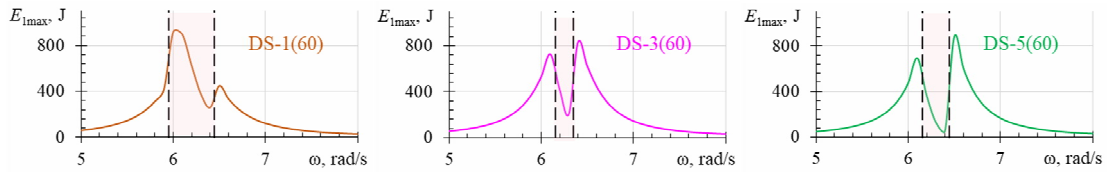


Fig. 4. The areas of bilateral and unilateral impacts for different double-sided vibro-impact nonlinear energy sinks with mass $m_2 = 60$ kg depending on the exciting force frequency

Fig. 5 shows the amplitude-modulated regime characteristics in detail. The upper envelope in red color in the plot of the time history of PS displacements is obtained using the Hilbert transform. Its frequency $\Omega = 0.31$ rad/s.

The analysis of the above allows us to formulate the following observations.

- Indeed, there is a lot of damper parameter sets that ensure the similar good mitigation of the PS vibrations. Table 2 and Fig. 2 clearly demonstrate this.

- A small changing in only one parameter can cause a significant change in the damper dynamics. Changing the clearance C in the variants SS-1(60) and SS-2(60) (see Table 2) gives a different motion picture (see Fig. 2).

- Attaching SSVI NES or DSVI NES to the PS does not change the behavior of the PS energy as a whole, which can be clearly seen in Fig. 2. However, the dynamics of the system movement is significantly different for these damper types. The “Regimes” rows in Table 2 show quiet motion with symmetrical impacts on both obstacles for the system with attached DSVI NES. In contrast, the system with attached SSVI NES demonstrates complex dynamics with both periodic and irregular motions. Fig. 5 presents the amplitude-modulated regime with bilateral impacts.

- It is important to emphasize that the bilateral impacts occur in rather narrow areas of the exciting force frequency located near the resonant one. For the system with DSVI NES attached, these areas are narrower, which can be clearly seen in Figs. 3 and 4.

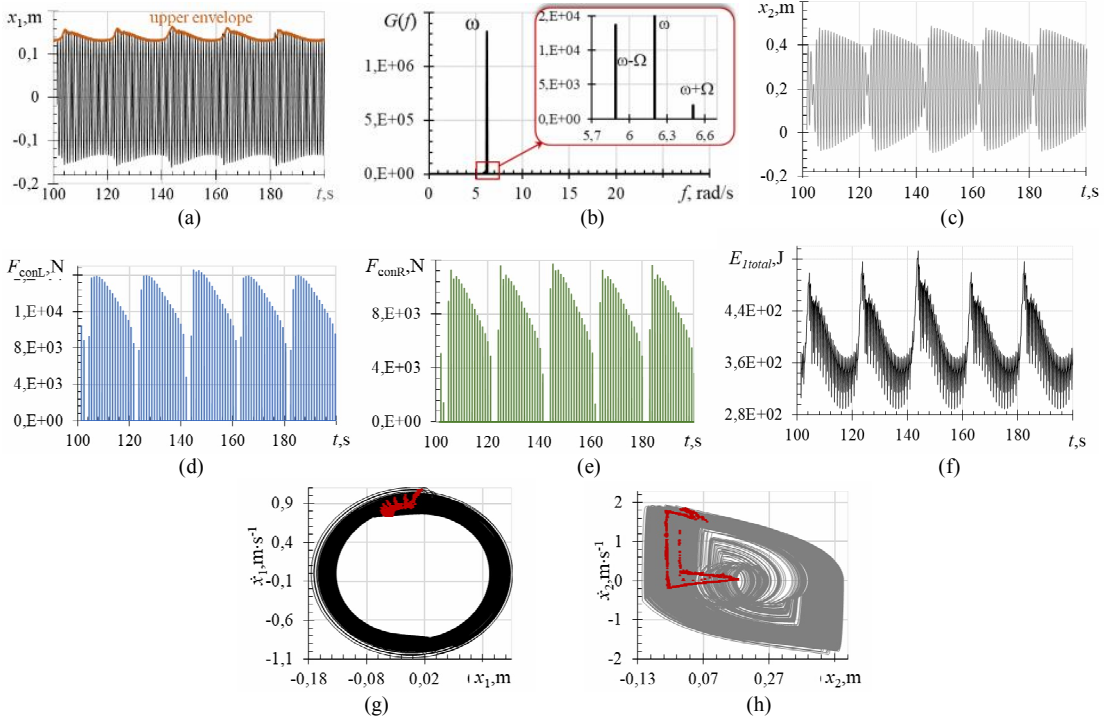


Fig. 5. Characteristics of the amplitude-modulated (AM) regime for the system with the damper of SS-2(60) variant at $\omega = 6.2$ rad/s. (a) The time history of the PS displacements. The frequency of the red upper envelope is $\Omega = 0.31$ rad/s. (b) Fourier spectrum for PS. (c) The time history of the damper displacements. (d) The contact impact forces at direct damper impacts on the PS. (e) The contact forces at damper impacts on the obstacle. (f) The total mechanical PS energy depending on time. (g) The phase trajectories and Poincaré map in red for PS. (h) The phase trajectories and Poincaré map in red for the damper

5. Dynamic behavior of the system with attached dampers of mass $m_2 = 40$ kg

The performance and dynamics of the system with DSVI NES and SSVI NES of mass $m_2 = 40$ kg attached to the PS have been discussed in detail in our previous work [18]. Optimization procedures allowed us to find several damper parameter sets that mitigate the PS vibrations well. In general, the pattern of the behavior of the PS energy is similar to that with dampers of mass $m_2 = 60$ kg. Fig. 6 shows the dependence of the maximum total energy of the PS with attached SSVI NESs and DSVI NESs of mass $m_2 = 40$ kg on the exciting force frequency.

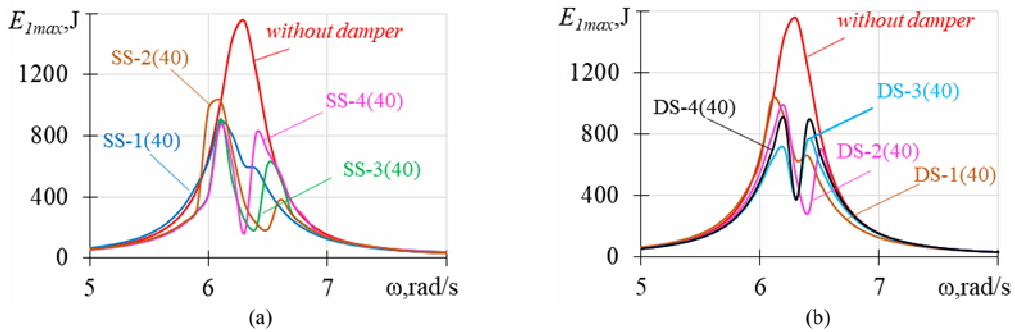


Fig. 6. Maximum total energy of the PS with different attached dampers of mass $m_2 = 40$ kg depending on the exciting force frequency; (a) for SSVI NES; (b) for DSVI NES

However, we observe a tendency to increase the clearance C and to decrease the damping coefficient c_2 especially pronounced for SSVI NES. Table 3 shows this trend.

Table 3

Tendency of increasing the clearance C and decreasing the damping coefficient c_2 with decreasing the damper masa

| Parameters | Variant | | | | | | | |
|---------------------------------------|----------|----------|----------|----------|----------|----------|----------|----------|
| | SS-1(40) | SS-2(40) | SS-3(40) | SS-4(40) | DS-1(40) | DS-2(40) | DS-3(40) | DS-4(40) |
| $c_2, \text{N}\cdot\text{s}/\text{m}$ | 232 | 76.7 | 64.1 | 42.6 | 232 | 64.8 | 97.6 | 74.5 |
| C, m | 0.300 | 0.518 | 0.644 | 0.771 | 0.158 | 0.238 | 0.260 | 0.276 |

6. Dynamic behavior of the system with attached dampers of mass $m_2=20 \text{ kg}$

Optimization procedures allowed us to find several damper parameter sets that provide a reasonably good mitigation of the PS vibrations even at a lower damper mass m_2 . However, as numerous tests have shown, the tendency for the clearance C to increase and the damping coefficient c_2 to decrease was increasingly strong. In addition, the dynamics of even DSVI NES is no longer calm; it becomes complex and exhibits irregular regimes. Let's look at these phenomena in more detail. Table 4 presents the characteristics of the four variants for SSVI NES and DSVI NES with optimized design. Table 4 demonstrates very large values of the clearance C and small values of the damping coefficient c_2 .

Table 4

Information about 4 variants of SSVI NES and DSVI NES of mass $m_2=20 \text{ kg}$ with optimized design

| Parameters | Variant | | | | | | | |
|---|--------------------------------------|-------------------------|------------------------|--|------------------------------|------------------------------|---|---|
| | SS-1(20) | SS-2(20) | SS-3(20) | SS-4(20) | DS-1(20) | DS-2(20) | DS-3(20) | DS-4(20) |
| $k_2, \text{N}/\text{m}$ | 205 | 225 | 125 | 198 | 697 | 699 | 678 | 679 |
| $c_2, \text{N}\cdot\text{s}/\text{m}$ | 42.1 | 35.3 | 28.9 | 36.0 | 19.2 | 19.6 | 13.9 | 10.3 |
| $D(I), \text{m}$ | 0.135 | 0.0154 | 0.0440 | 0.759 | 0.365 | 0.0227 | 0.0127 | 0.00544 |
| C, m | 0.758 | 0.908 | 0.839 | 0.871 | 0.653 | 0.650 | 0.728 | 0.774 |
| $E_{1\text{max}}, \text{J}$ at $\omega=6.3 \text{ rad/s}$ | 586 | 573 | 672 | 526 | 200 | 204 | 134 | 101 |
| Regimes | $T_{0,0}$ $T_{1,0}$ $2T_{2,2}$ | $T_{1,0}$ $3T_{3,1}$ | $T_{1,0}$ $T_{1,1}$ | $T_{0,0}$ $T_{1,0}$ $2T_{2,2}$ $2T_{1,0}$ | $T_{0,0}$ $T_{1,1}$ AM | $T_{0,0}$ $T_{1,1}$ AM | $T_{0,0}$ $T_{1,1}$ $3T_{2,2}$ $T_{1,1}$ with rare bursts AM | $T_{0,0}$ Chaotic $T_{1,1}$ $3T_{2,2}$ AM |

Fig. 7 presents the dependence of the maximum total energy $E_{1\text{max}}$ of the PS on the exciting force frequency for these four variants.

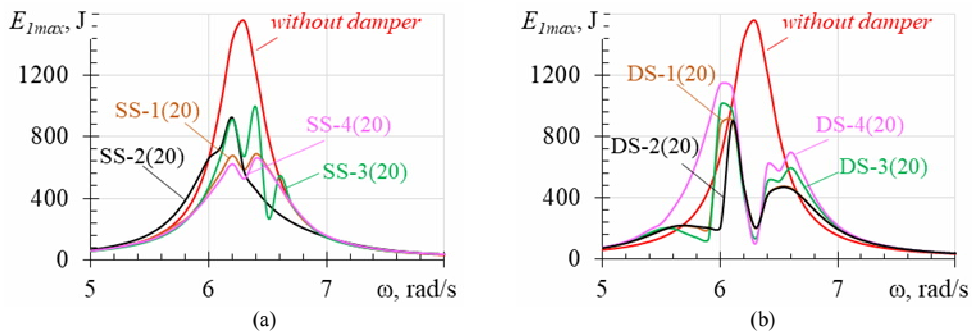


Fig. 7. Maximum total energy of the PS with different attached dampers of mass $m_2=20 \text{ kg}$ depending on the exciting force frequency; (a) for SSVI NES; (b) for DSVI NES

The areas of bilateral impacts remain narrow.

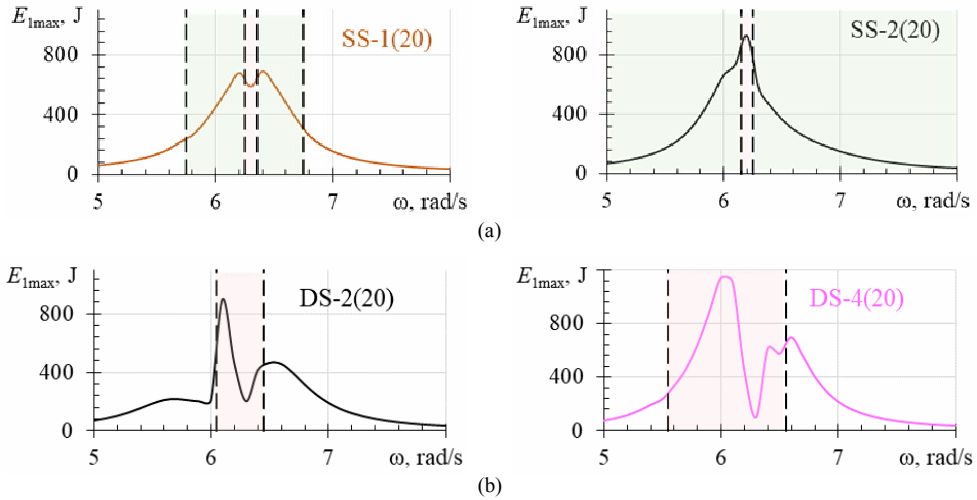


Fig. 8. The areas of bilateral and unilateral impacts for different vibro-impact nonlinear energy sinks with mass $m_2=20$ kg depending on the exciting force frequency: (a) for SSVI NES; (b) for DSVI NES

Let's show the chaotic motion that occurs in the system with attached DSVI NES of DS-4(20) variant at low exciting force frequency $\omega = 5.7$ rad/s. Fig. 9 presents its characteristics.

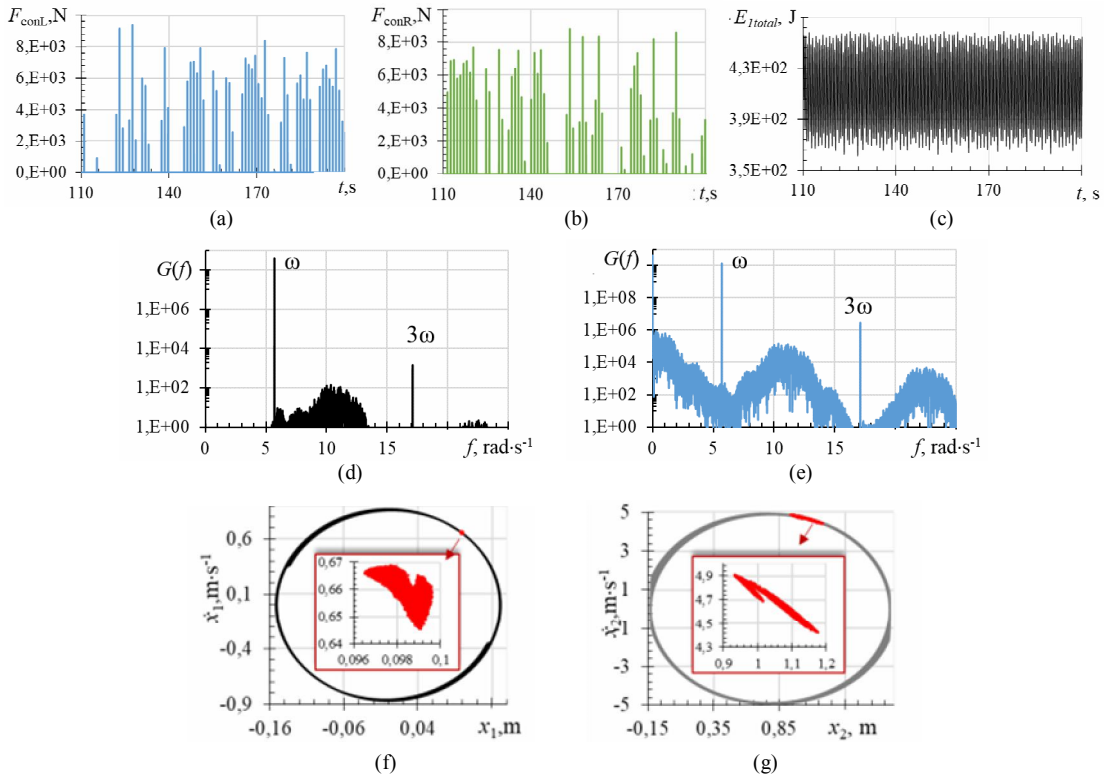


Fig. 9. Characteristics of chaotic motion of the system with variant DS-4(20) attached to PS at exciting force frequency $\omega = 5.7$ rad/s. (a) Contact impact forces at impacts on the left obstacle. (b) Contact impact forces at impacts on the right obstacle. (c) Total PS energy depending on time. (d) Fourier spectrum for PS in logarithmic scale. (e) Fourier spectrum for the damper in logarithmic scale. (f) Phase trajectories with Poincaré map in red for PS. (g) Phase trajectories with Poincaré map in red for the damper

This motion exhibits broad continuous Fourier spectra for both PS and the damper. The Poincaré maps have the shape of smears. This is typical for chaotic movement.

7. Dynamic behavior of the system with attached dampers of mass $m_2 = 10$ kg

In world scientific literature it is often recommended to use NES with a small mass m_2 , which is 1% of the PS mass m_1 . Therefore, it is worthwhile to see how such a NES reduces the PS vibrations and what is its optimized design.

Numerous numerical experiments have shown that the trend noted above is developing. The clearance C increases to huge values; the damping coefficient c_2 is greatly reduced. The dynamics becomes complex for both SSVI NES and DSVI NES; the symmetry of the impacts for DSVI NES is broken. However, despite these phenomena, VI NESs with these parameters provide good mitigation of the PS vibrations. Let’s show in detail the dynamic behavior of the system with dampers of mass $m_2 = 10$ kg attached to PS. Table 5 presents the characteristics of the four variants for SSVI NES and DSVI NES with optimized design.

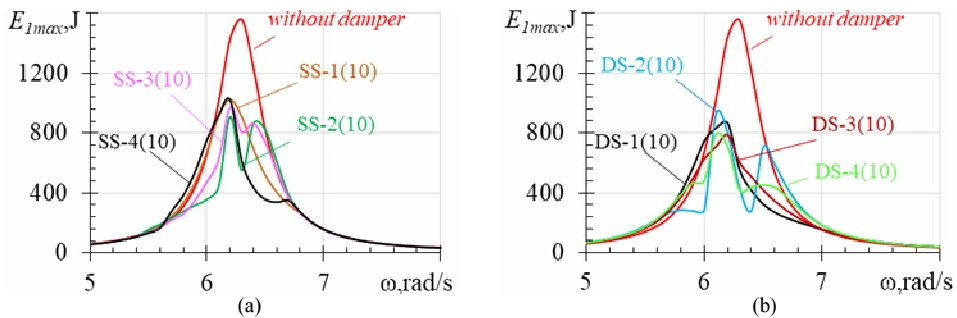


Fig. 10. Maximum total energy of the PS with different attached dampers of mass $m_2 = 10$ kg depending on the exciting force frequency; (a) for SSVI NES; (b) for DSVI NES

Table 5 shows huge values of the clearance C and very small values of the damping coefficient c_2 . The rows with the title “Regimes” demonstrate the presence of different irregular motions in the system with these VI NESs attached to the PS. Fig. 10 presents the dependence of the maximum total energy E_{1max} of the PS on the exciting force frequency for these four variants.

Table 5

Information about 4 variants of SSVI NES and DSVI NES of mass $m_2 = 10$ kg with optimized design

| Parameters | Variant | | | | | | | |
|--|-------------------------------|-------------------------------|-------------------------------|-------------------------------|--------------------|--------------------|--------------------|--|
| | SS-1(10) | SS-2(10) | SS-3(10) | SS-4(10) | DS-1(10) | DS-2(10) | DS-3(10) | DS-4(10) |
| $k_2, \text{N/m}$ | 133 | 98.8 | 103 | 127 | 354 | 414 | 387 | 428 |
| $c_2, \text{N}\cdot\text{s/m}$ | 18.3 | 6.88 | 13.4 | 7.78 | 7.14 | 14.8 | 8.57 | 12.6 |
| $D (V), \text{m}$ | 0.135 | 0.152 | 0.171 | 0.207 | 0.0194 | 0.185 | 0.149 | 0.0276 |
| C, m | 0.975 | 2.01 | 1.30 | 1.67 | 1.037 | 0.735 | 0.985 | 0.799 |
| E_{1max}, J at $\omega = 6.3 \text{ rad/s}$ | 428 | 603 | 411 | 560 | 428 | 603 | 411 | 560 |
| Regimes | $T,0,0$ $T,1,0$ Chaotic | $T,0,0$ $T,1,0$ Chaotic | $T,0,0$ $T,1,0$ Chaotic | $T,0,0$ $T,1,0$ Chaotic | $T,0,0$ Chaotic | $T,0,0$ $T,1,1$ | $T,0,0$ Chaotic | $T,0,0$ Chaotic $T,1,1$ with rare bursts $T,1,1$ AM |

The areas of bilateral impacts are extremely narrow (Fig. 11).

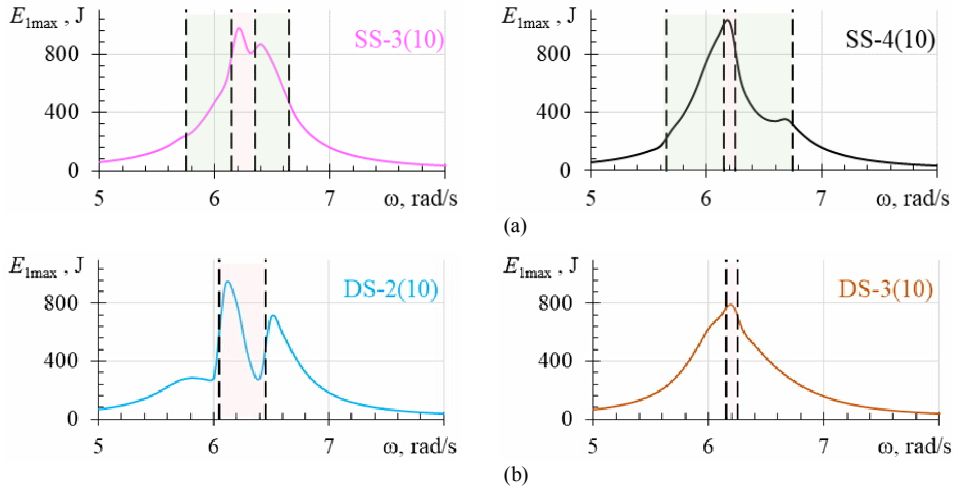


Fig. 11. The areas of bilateral and unilateral impacts for different variants of VI NESs with mass $m_2=10$ kg depending on the exciting force frequency: (a) for SSVI NES; (b) for DSVI NES

As can be seen from Fig. 11 (a) for the SSVI NES, there are some regions with unilateral damper impacts on the PS directly. Fig. 11 (b) shows that the DSVI NES operates as a nonlinear vibro-impact device in an extremely narrow region of the exciting force frequency. The system performs shockless $T,0,0$ movement throughout the rest of the exciting force frequency range. The DSVI NES operates as a linear damper without the nonlinearity that occurs when hitting the obstacles. The SSVI NES operates as a nonlinear vibro-impact device over a wider range of exciting force frequencies, but it makes unilateral impacts on the PS directly and does not impact the obstacle. Generally speaking, the SSVI NES can be thought of as a double-sided device, only asymmetrical, since it strikes the barriers from two sides – the obstacle on the right and the PS directly on the left.

Let’s show the characteristics of chaotic movement for DS-4(10) at exciting force frequency $\omega=6.1$ rad/s (Fig. 12). The picture of this chaotic movement is similar to the picture of chaotic movement in Fig. 9 for damper with mass $m_2=20$ kg, but the asymmetry of the left and right contact forces has increased. Figs. 12 (a), (b) clearly show asymmetry of the impacts on the left (Fig. 12, (a)) and on the right (Fig.12, (b)) obstacles. The wide continuous Fourier spectra (Figs. 12, (d), (e)) are typical for chaotic motion. The shape of Poincaré maps in the form of smears are also typical for the chaotic motion.

It is worth emphasizing that low-mass dampers are good in mitigating the PS vibrations when their optimal parameters have unusual non-standard values, namely large clearance C and small damping coefficient c_2 . When they have “normal” usual values, the mitigation is very weak, it is almost non-existent. Let’s show the performance of the SSVI NES and DSVI NES with such design as an example. The damper parameters are presented in Table 6. Fig. 13 shows the behavior of the PS energy with attached dampers with usual “normal” parameters versus the PS energy with attached dampers with unusual “strange” parameters. The areas of bilateral impacts for these dampers are also narrow and located near the resonant frequency. The impacts are symmetrical for DSVI NES and asymmetrical for SSVI NES. The unilateral direct impacts of the SSVI NES on the PS occur throughout the rest of the exciting force frequency range. A system with the attached DSVI NES performs shockless motion over the entire exciting force frequency range, except for a narrow band of bilateral impacts. The DSVI NES operates in the shockless zone as a linear damper.

Table 6
The “normal” parameters of SSVI NES and DSVI NES with mass $m_2=10$ kg.

| Paramters | Variant | |
|---------------|----------|----------|
| | SS-5(10) | DS-5(10) |
| k_2 , N/m | 215 | 215 |
| c_2 , N·s/m | 250 | 132 |
| D (V), m | 0.01 | 0.1 |
| C , m | 0.1 | 0.1 |

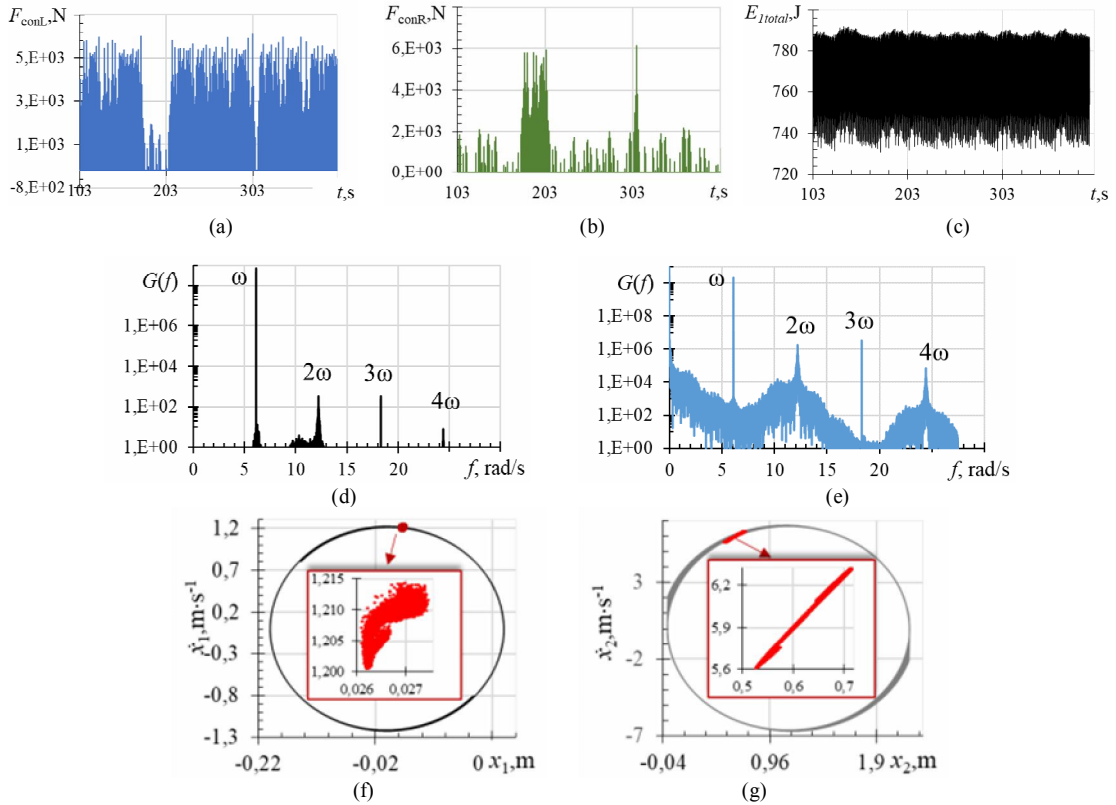


Fig. 12. Characteristics of chaotic motion of the system with variant DS-4(10) attached to PS at exciting force frequency $\omega = 6.1$ rad/s. (a) Contact impact forces at impacts on the left obstacle. (b) Contact impact forces at impacts on the right obstacle. (c) Total energy of PS. (d) Fourier spectrum for PS in logarithmic scale. (e) Fourier spectrum for the damper in logarithmic scale. (f) Phase trajectories with Poincaré map in red for PS. (g) Phase trajectories with Poincaré map in red for damper

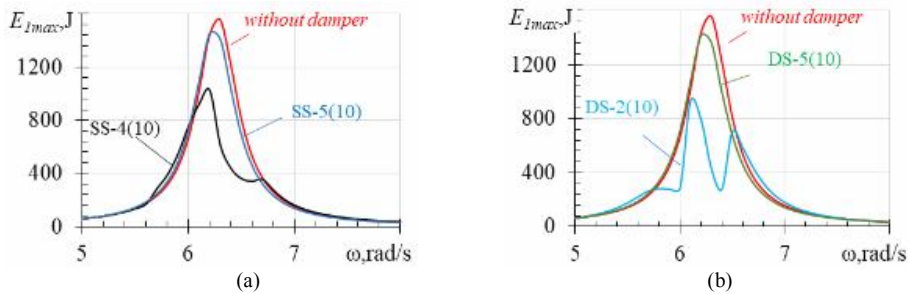


Fig. 13. Maximum total energy of the PS when dampers of mass $m_2 = 10$ kg with usual “normal” parameters are attached to it: (a) for SSVI NES; (b) for DSVI NES

8. Conclusions

Numerous numerical experiments, the results of which are presented above in Figures and Tables, allow us drawing the following conclusions.

- There are many sets of damper parameters that provide similar high efficiency in reducing the PS vibrations.
- Optimization procedures produce ambiguous results and allow for a great deal of arbitrariness.
- Symmetrical double-sided and asymmetrical single-sided vibro-impact nonlinear sinks with optimized design provide the similar efficiency in mitigating the PS vibrations. From this point of view, none of these damper types offers any advantages.

- The NESs with larger mass provide good mitigation of the PS vibrations when they have “normal” usable design. When the damper mass is reduced, its efficiency is preserved, but the optimal parameters providing such efficiency become very “strange”, namely: the clearance becomes huge and the damping coefficient becomes very small.

- The system dynamics changes when the damper mass is reduced. When the damper has a larger mass, a system with a DSVI NES attached to the PS exhibits quiet periodic dynamics with symmetrical impacts on the left and right obstacles. A system with a lighter DSVI NES exhibits irregular motions with asymmetrical impacts on the left and right obstacles.

- The SSVI NES hits both right obstacle and the PS directly. From this point of view, it can be considered as double-sided device, since it hits the barriers on two sides. However, these impacts are asymmetrical. Dynamics of SSVI NES is complex with different both periodic and irregular movements.

- Bilateral impacts occur in a very narrow range of the exciting force frequency. The narrow areas of bilateral impacts are located near resonance. In the rest frequency range, the system with DSVI NES performs a shockless motion without any impacts. The DSVI NES acts as a linear damper because there is no nonlinearity created by impacts. The SSVI NES also exhibits a narrow region of bilateral impacts, but over a wider frequency range makes unilateral direct impacts on the PS.

REFERENCES

1. Ding H., Chen L. Q. Designs, analysis, and applications of nonlinear energy sinks //Nonlinear Dynamics. – 2020. – T. 100. – №. 4. – C. 3061-3107. doi:10.1007/s11071-020-05724-1
2. Saeed A. S., Abdul Nasar R., AL-Shudeifat M. A. A review on nonlinear energy sinks: designs, analysis and applications of impact and rotary types //Nonlinear Dynamics. – 2023. – T. 111. – №. 1. – C. 1-37. doi:10.1007/s11071-022-08094-y
3. Wierschem, Nicholas E.; Spencer, Billie F., Jr. Targeted energy transfer using nonlinear energy sinks for the attenuation of transient loads on building structures, Newmark Structural Engineering Laboratory Report Series 045. 600. <https://www.ideals.illinois.edu/items/89701>
4. Gendelman O. V. Transition of energy to a nonlinear localized mode in a highly asymmetric system of two oscillators //Nonlinear dynamics. – 2001. – T. 25. – C. 237-253. doi:10.1007/978-94-017-2452-4_13
5. Vakakis A. F., Gendelman O. Energy pumping in nonlinear mechanical oscillators: part II—resonance capture //J. Appl. Mech. – 2001. – T. 68. – №. 1. – C. 42-48. doi:10.1115/1.1345525
6. Weidemann T, Bergman LA, Vakakis AF, Krack M. Energy Transfer and Localization in a Forced Cyclic Chain of Oscillators with Vibro-Impact Nonlinear Energy Sinks. – 2024. doi:10.21203/rs.3.rs-4691661/v1
7. Li, W., Wang, Z., Brennan, M. J., & Yang, T. Design and optimization of a two-degrees-of-freedom single-sided vibro-impact nonlinear energy sink for transient vibration suppression of a thin plate //Journal of Sound and Vibration. – 2024. – T. 587. – C. 118512. doi:10.1016/j.jsv.2024.118512
8. Wang, Y., Zhang, J., Wang, W., Mao, G., Hong, J., & Fang, B. Influence of the VI-NES on the resonance response regime and amplitude-frequency characteristics for the duffing system //Nonlinear Dynamics. – 2024. – C. 1-23. doi:10.1007/s11071-024-10253-2
9. Li, H., Li, S., Zhang, Z., Xiong, H., & Ding, Q. Effectiveness of vibro-impact nonlinear energy sinks for vibration suppression of beams under traveling loads //Mechanical Systems and Signal Processing. – 2025. – T. 223. – C. 111861. doi:10.1016/j.ymsp.2024.111861
10. Gzal, M. O., Gendelman, O. V., Bergman, L. A., & Vakakis, A. F. How internal vibro-impact nonlinearities yield enhanced vibration mitigation //Nonlinear Dynamics. – 2024. – T. 112. – №. 20. – C. 17683-17708. doi:10.1007/s11071-024-09902-3
11. Gzal, M. O., Gendelman, O. V., Bergman, L. A., & Vakakis, A. F. Enhanced seismic mitigation through energy management using nonlinear energy sinks with clearance-contacts. – 2024. doi:10.21203/rs.3.rs-4893272/v1
12. Lu, Z., Wang, Z., Zhou, Y., & Lu, X. Nonlinear dissipative devices in structural vibration control: A review //Journal of Sound and Vibration. – 2018. – T. 423. – C. 18-49. doi:10.1016/j.jsv.2018.02.052
13. Kang X, Tang J, Xia G, Wei J, Zhang F, Sheng Z. Design, optimization, and application of nonlinear energy sink in energy harvesting device //International Journal of Energy Research. – 2024. – T. 2024. – №. 1. – C. 2811428. doi:10.1155/2024/2811428
14. Bazhenov V. A., Pogorelova O. S., Postnikova T. G. Comparison of two impact simulation methods used for nonlinear vibroimpact systems with rigid and soft impacts //Journal of Nonlinear Dynamics. – 2013. – T. 2013. – №. 1. – C. 485676. doi:10.1155/2013/485676
15. Bazhenov V, Pogorelova O, Postnikova T. Crisis-Induced Intermittency and Other Nonlinear Dynamics Phenomena in Vibro-impact System with Soft Impact. In: Holm Altenbach, Marco Amabili, Yuri V. Mikhlin, ed. Nonlinear Mechanics of Complex Structures. Springer Nature; 2021:185-203. doi:10.1007/978-3-030-75890-5_11
16. Johnson KL. Contact Mechanics. Cambridge University Press; 1987.
17. Goldsmith W. The Theory and Physical Behaviour of Colliding Solids. Edward Arnold Publishers Ltd; 1960
18. Lizunov P., Pogorelova O., Postnikova T. Comparison of the performance and dynamics of the asymmetric single - sided and symmetric double - sided vibro - impact nonlinear energy sinks with optimized designs //International Journal of Mechanical System Dynamics. – 2024. doi:10.1002/msd2.12126
19. Lizunov P., Pogorelova O., Postnikova T. Vibro-impact damper dynamics depending on system parameters. Research Square. Published online 2023. doi:10.21203/rs.3.rs-2786639/v1

20. Lizunov P., Pogorelova O., Postnikova T. The influence of various optimization procedures on the dynamics and efficiency of nonlinear energy sink with synergistic effect consideration //Physica D: Nonlinear Phenomena. – 2024. – Т. 463. – С. 134167. doi:10.1016/j.physd.2024.134167
21. Lizunov P., Pogorelova O., Postnikova T. Optimization of a vibro-impact damper design using MATLAB tools //Strength of Materials and Theory of Structures. – 2024. – №. 112. – С. 3-18. doi:10.32347/2410-2547.2024.112.3-18
22. Kumar R., Kuske R., Yurchenko D. Exploring effective TET through a vibro-impact nonlinear energy sink over broad parameter regimes //Journal of Sound and Vibration. – 2024. – Т. 570. – С. 118131. doi:10.1016/j.jsv.2023.118131
23. AL-Shudeifat M. A., Saeed A. S. Comparison of a modified vibro-impact nonlinear energy sink with other kinds of NESs //Meccanica. – 2021. – Т. 56. – С. 735-752. doi:10.1007/s11012-020-01193-3
24. Gendelman O. V. Targeted energy transfer in systems with external and self-excitation //Proceedings of the Institution of Mechanical Engineers, Part C: Journal of Mechanical Engineering Science. – 2011. – Т. 225. – №. 9. – С. 2007-2043. doi:10.1177/0954406211413976

Стаття надійшла 22.09.2024

Лізунов П.П., Погорелова О.С., Постнікова Т.Г., Геращенко О.В.

ВПЛИВ МАСИ НА ЕФЕКТИВНІСТЬ ТА ДИНАМІКУ ОДНОБІЧНИХ ТА ДВОБІЧНИХ ВІБРОУДАРНИХ НЕЛІНІЙНИХ ПОГЛИНАЧІВ ЕНЕРГІЇ

У цій статті досліджується ефективність асиметричних односторонніх і симетричних двосторонніх віброударних нелінійних поглиначів енергії (SSVI NES і DSVI NES), тобто віброударних демпферів, у зменшенні небажаних коливань важкої основної конструкції (PS), до якої ці демпфери прикріплені. Також досліджено динамічну поведінку цієї віброударної системи. Ефективність демпфера і поведінка системи досліджуються для демпферів з чотирма різними масами, оскільки оптимізація інших параметрів демпфера проводиться для заздалегідь визначеній масі. Показано вплив зміни маси демпфера на його ефективність і динамічну поведінку системи. Демпфери з різною масою і оптимальною конструкцією демонструють подібну високу ефективність у зменшенні коливань PS, але оптимальна конструкція демпфера з меншою масою має незвичні параметри, а саме: великий зазор і малий коефіцієнт демпфування. SSVI NES ударає не тільки перешкоду, жорстко зв'язану з PS, але й безпосередньо PS. З цієї точки зору його можна вважати двостороннім DSVI NES, тільки асиметричним. DSVI NES ударає ліву і праву перешкоди, жорстко зв'язані з PS. Області двосторонніх ударів вузькі і розташовані поблизу резонансної частоти збуджуючої сили. У решті частотного діапазону SSVI NES здійснює односторонні прямі удари по PS; DSVI NES здійснює безударний рух без будь-яких ударів і працює в цьому діапазоні частот як лінійний демпфер без будь-якої нелінійності.

Численні чисельні тести забезпечили можливість показати динаміку системи з 36 різними демпферами, а саме для чотирьох мас, для двох типів демпферів для кожної маси і для декількох варіантів оптимальної конструкції демпфера. Оптимальна конструкція не єдина, вона може мати багато варіантів, оскільки існує безліч наборів параметрів демпферів, які забезпечують подібне зменшення коливань основної конструкції. Тому сама процедура оптимізації не дає і не може дати однозначного результату, допускає велику довільність у її виконанні і вимагає від виконавця великого досвіду і майстерності.

Ключові слова: нелінійний поглинач енергії, демпфер, віброударний, однобічний, двобічний, оптимізація, двосторонні удари.

Lizunov P.P., Pogorelova O.S., Postnikova T.G., Gerashchenko O.V.

INFLUENCE OF MASS ON THE EFFICIENCY AND DYNAMICS OF SINGLE-SIDED AND DOUBLE-SIDED VIBRO-IMPACT NONLINEAR ENERGY SINKS

This paper studies the efficiency of the asymmetric single-side and symmetric double-sided vibro-impact nonlinear energy sinks (SSVI NES and DSVI NES), that is, vibro-impact dampers, in mitigating unwanted vibrations of the heavy primary structure (PS) to which these dampers are attached. The dynamic behavior of this vibro-impact system is also investigated. The damper efficiency and system behavior are studied for dampers with four different masses, as optimization is carried out for other damper parameters at a predetermined mass. The effect of the damper mass changing on its efficiency and system dynamic behavior is shown. The dampers with different masses and optimal design exhibit similar high efficiency in mitigating the PS vibrations, but the optimal design of the dampers with lower mass has unusual parameters, namely the huge clearance and small damping coefficient. The SSVI NES hits not only the obstacle hardwired to the PS but also the PS directly. From this point of view, it can be considered as double-sided DSVI NES only asymmetric. The DSVI NES hits the left and right obstacles rigidly connected with PS. The regions of bilateral impacts are narrow and located near the resonant frequency of the exciting force. In the rest of the frequency range, the SSVI NES makes unilateral direct impacts on the PS; the DSVI NES performs shockless motion without any impacts and operates in this frequency range as a linear damper without any nonlinearity.

The numerous numerical tests were able to show the system dynamics with 36 different dampers, namely for four masses, for two damper types for each mass, and for several variants of the optimal damper design. The optimal design is not unique; it can have many variants, since there is a lot of damper parameter sets that provide similar mitigation of the main structure vibrations. Therefore, optimization procedure itself does not and cannot give an unambiguous result, allows for great arbitrariness in its execution and requires great experience and skill from the performer.

Keywords: nonlinear energy sink, damper, vibro-impact, single-sided, double-sided, optimization, bilateral impacts.

УДК 539.3

Лізунов П.П., Погорелова О.С., Постнікова Т.Г., Геращенко О.В. Вплив маси на ефективність та динаміку однобічних та двобічних віброударних нелінійних поглиначів енергії // Опір матеріалів і теорія споруд: наук.-тех. збірн. – К.: КНУБА. 2024. – Вип. 113. – С. 3-17. – Англ.

Ефективність асиметричних односторонніх і симетричних двосторонніх віброударних нелінійних поглиначів енергії тобто віброударних демпферів, для зменшення небажаних коливань основної конструкції є досить високою і подібною для демпферів з різною масою і конструкцією. Однак їхня динамічна поведінка відрізняється. Оптимальна конструкція демпферів з меншою масою має незвичний, «дивний» набір параметрів. Області двостороннього впливу демпфера на обидва бар'єри вузькі і розташовані поблизу резонансної частоти збуджуючої сили.

UDC 539.3

Lizunov P.P., Pogorelova O.S., Postnikova T.G., Gerashchenko O.V. Influence of mass on the efficiency and dynamics of single-sided and double-sided vibro-impact nonlinear energy sinks // Strength of Materials and Theory of Structures: Scientific-and-technical collected articles. – K.: KNUBA. 2024. – Issue113. – P. 3-17.

The efficiency of the asymmetric single-sided and symmetric double-sided vibro-impact nonlinear energy sinks, that is, or vibro-impact dampers, for mitigating unwanted vibrations of the main structure are quite high and similar for dampers with different masses and designs. However, its dynamic behavior is different. The optimal design of the dampers with lower mass has unusual, "strange" parameter set. The regions of bilateral damper impacts on the both barriers are narrow and located near the resonant frequency of the exciting force.

Tabl. 6. Figs. 13. Refs. 24.

Автор (науковий ступінь, вчене звання, посада): доктор технічних наук, професор, завідувач кафедри будівельної механіки КНУБА, директор НДІ будівельної механіки ЛІЗУНОВ Петро Петрович

Адреса робоча: 03680 Україна, м. Київ, проспект Повітряних Сил 31, Київський національний університет будівництва і архітектури

Робочий тел.: +38(044) 245-48-29

Мобільний тел.: +38(067)921-70-05

E-mail: lizunov@knuba.edu.ua

ORCIDID: <http://orcid.org/0000-0003-2924-3025>

Автор (науковий ступінь, вчене звання, посада): кандидат фізико-математичних наук, старший науковий співробітник, провідний науковий співробітник НДІ будівельної механіки ПОГОРЕЛОВА Ольга Семенівна

Адреса робоча: 03680 Україна, м. Київ, проспект Повітряних Сил 31, Київський національний університет будівництва і архітектури

Робочий тел.: +38(044) 245-48-29

Мобільний тел.: +38(067) 606-03-00

E-mail: pogos13@ukr.net

ORCID ID: <http://orcid.org/0000-0002-5522-3995>

Автор (науковий ступінь, вчене звання, посада): кандидат технічних наук, старший науковий співробітник, провідний науковий співробітник НДІ будівельної механіки ПОСТНІКОВА Тетяна Георгіївна

Адреса робоча: 03680 Україна, м. Київ, проспект Повітряних Сил 31, Київський національний університет будівництва і архітектури

Робочий тел.: +38(044) 245-48-29

Мобільний тел.: +38(050) 353-47-19

E-mail: postnikova.tg@knuba.edu.ua

ORCID ID: <https://orcid.org/0000-0002-6677-4127>

Автор (науковий ступінь, вчене звання, посада): кандидат технічних наук, старший науковий співробітник, зав. відділом НДІ будівельної механіки ГЕРАЩЕНКО Олег Валерійович.

Адреса робоча: 03680 Україна, м. Київ, проспект Повітряних Сил 31, Київський національний університет будівництва і архітектури

Робочий тел.: +38(044)248-30-40

Мобільний тел.: +38(095)661-6052

E-mail: olg.guera@ukr.net

ORCID ID: <http://orcid.org/0000-0003-1951-4805>